Comparison of Nonlinear Filtering Methods for Battery State of Charge Estimation

A Thesis

Submitted to the Graduate Faculty of the
University of New Orleans
in partial fulfillment of the
requirements for the degree of

Masters of Science
in
Electrical Engineering

by

Klaus Zhang

B.S. Pennsylvania State University, 2011

May 2014

Abstract

In battery management systems, the State of Charge, obtained from voltage and current measurements, is a figure of merit. The estimation of State of Charge is challenging due to the nonlinear behavior of the battery, measurement noise, and the trade-off between accuracy and energy usage in selecting the sample rate. Additionally, for the purposes of eletrical-system design, an electrical-circuit battery model is useful, which presents additional filtering difficulties when compared to presently-used analytical models [wordy]. This thesis investigated the performance of various nonlinear filters for estimating the State of Charge using an electrical-circuit battery model.

Table of Contents

Chapter 1

Introduction

Batteries, particularly rechargeable ones, are used extensively in daily life. They provide the energy for such electrical systems as communication, automotive, and renewable power systems, among others. In order to design for and operate these systems, an accurate battery model and a means of simulating the model efficiently is needed. For example, modern battery charge and health management schemes use high-fidelity battery models to track the state of charge (SOC) and state of health (SOH); this information is then used to predict and optimize runtime of the battery. However, most batteries have nonlinear capacitive effects, which require the use of a nonlinear filter. This thesis provides one possible solution to this problem by choosing an appropriate battery model and testing the speed and accuracy of various nonlinear filters in determining the SOC.

1.1 Electrical Characteristics of Rechargeable Batteries

A high-fidelity battery model has to accurately reproduce the various characteristics of the battery. The characteristics included in most models are the capacity and the state of charge. More accurate models include nonlinear effects, such as the rate-capacity effect and the recovery effect, along with self-discharge and the effects of ambient temperature. The dynamic electrical attributes, such as the current-voltage (i-v) characteristics and transient

responses, can also be modeled.

The capacity of a battery is the amount of electric charge it can store, measured in the SI unit Ampere-hours (Ah). Commonly, for rechargeable battery specifications, the subunit milliampere-hour (mAh) is used. Due to the electrochemical nature of batteries, a battery's available capacity decreases as the rate of discharge increases. Therefore, the capacity for a battery is typically stated for a given discharge rate. For lead-acid batteries, this diminishing capacity with increasing discharge rate is known as Peukert's law, which states that for a one-ampere discharge rate [1]

$$C_p = I^k t, \tag{1.1}$$

where C_p is the capacity at a one-ampere discharge rate in Ah, I is the discharge current in A, t is the time to discharge the battery in hours, and $k >= 1$ is the dimensionless Peukert constant, typically between 1.1 and 1.3 for a lead-acid battery. The constant k only equals unity for an ideal accumulator, so for real batteries, k is always greater than unity. Thus, for a given increase in the discharge current, the discharge time decreases by a proportionally greater amount. Therefore, the effective, or available, capacity Ct is reduced. For a general battery, this effect is known as the rate-capacity effect. Related to this is the recovery effect, so called because when a battery is allowed to rest during an idle period, the battery "recovers" available capacity previously lost during discharge due to the rate-capacity effect.

Both the rate-capacity effect and the recovery effect can be explained by the electrochemical nature of the battery. During discharge the concentration of the active material around the electrode is depleted and the active materials in the depletion region move towards the electrode to reduce the concentration gradient [2]. Because the speed at which the concentration gradient is equalized is limited, the faster the rate of discharge, the less active material has been replenished, resulting in a decrease in the capacity. Likewise, when the battery is allowed to rest, the active material gradient has additional time to equalize and increase the

available capacity.

Closely related to the capacity is the SOC. This thesis defines it as the ratio between the remaining capacity and the maximum capacity, with both capacities measured using the amount of active material within the battery. This definition then denotes the proportion of remaining chemical energy rather the available energy and is unaffected by the rate-capacity and recovery effects. Note that a fully charged battery has an SOC of unity and a fully discharged battery has an SOC of zero, regardless of the available capacity. Additionally, it is convenient to establish the relationship between the SOC of the battery and its open-circuit voltage V_{OC}, which is useful for simulation of the i-v characteristics and transient responses. V_{OC} can be thought as the limit of the measured battery voltage after recovery.

Other more minor effects that are usually incorporated into models are self-discharge, the effect of ambient temperature, and aging. Self-discharge refers to an idle battery decreasing its SOC over time due to internal chemical reactions. It is dependent on the type of battery, SOC, ambient temperatures, and other factors. The ambient temperature has effects on the internal resistance of the battery and the self-discharge rate. Commonly, the battery is designed to operate with a narrow range of temperatures. Below the operating temperature range, the internal resistance increases, decreasing the capacity. Above the operating range, the internal resistance decreases, not only increasing the capacity but also the self-discharge rate; thus, the actual capacity is lowered due to the increased self-discharge. Aging refers to the decrease in battery performance measures, such as capacity, self-discharge, and internal resistance, over time due to unwanted chemical reactions. In practice, aging is indicated by the SOH, defined as the ratio between the current maximum capacity and that of a new battery. The SOH threshold at which the battery performance is considered too degraded varies by application.

[Where does this go?] This thesis studied the prediction of the SOC of a battery using noisy measurements of its current and voltage. To do so accurately for a general load, incorporation

of the rate-capacity and recovery effects as well as the transient i-v characteristics is desirable. Furthermore, it is useful to have a model easily tunable for different battery types. The following section reviews the characteristics of different battery models and chooses the one most suitable for the purposes of this study.

1.2 Battery Models

Battery models can be divided into five categories, namely electrochemical, computational intelligence, analytical, stochastic, and electrical-circuit. The remainder of this section reviews each type and determines the most suitable battery model for this study..

1.2.1 Electrochemical

Electrochemical models are describe the chemical processes that place in the battery in great detail. These are generally the most accurate, but they require in-depth knowledge of the chemical processes to create and impose large computational costs [3]. One of the most widely known electrochemical models was developed by Doyle, Fuller, and Newman for lithium and lithium-ion batteries using noninvasive voltage-current cycling experiments [4–6]. It consists of six coupled, nonlinear differential equatons that capture lithium diffusion dynamics and charge transfer kinetics. The model is able to predict i-v response and provides a design guide for thermodynamics, kinetics, and transport across electrodes. A implementation of their model in Fortran, called Dualfoil, is available for free online.[1] The program needs more than 60 parameters along with the load profile in order to compute the battery properties. Setting the parameters requires detailed knowledge of the battery, but the result of the program is highly accurate. Other battery models are often compared to it rather than to experimental

[1] J. Newman, *Fortran programs for the simulation of electrochemical systems*, `http://www.cchem.berkeley.edu/jsngrp/fortran.html`, 1998.

results.

1.2.2 Computational Intelligence

Computational intelligence is a brance of computer science interested in problems that require the intelligence of humans and animals to solve. One of the earliest definitions by Bezdek states that computational intelligent systems use pattern recognition on low-level, numerical data and do not use knowledge as with artificial intelligence [8, 9]. Methods such as neural networks, fuzzy systems, and evolutionary computation are commonly classified as computational intelligence. Battery models using such methods as neural networks [10, 11], support vector machines [12], and hybrid neural-fuzzy models [13] have been studied. These models learn the nonlinear relationships between battery properties, such as SOC, current, voltage, and temperature, through a computationally costly training process. However, once trained, they incur a much lower cost and can achieve comparable accuracy to electrochemical models.

1.2.3 Analytical

[Needs rewrite to include more detail, eg equations]

1.2.3.1 Peukert's Law

Analytical models are simplified electrochemical models that trade off accuracy for simplicity. One of the simplest such models is Peukert's law, described above. It is able to model the rate-capacity effect but not the recovery effect. More complicated models, such as the kinetic battery model and the diffusion model, are able to describe both the rate-capacity effect and the recovery effect. However, the current examples of analytical models cannot describe the transient i-v characteristics of batteries.

1.2.3.2 Kinetic Battery Model

The kinetic battery model (KiBaM), initially created for large lead-acid batteries, describes the battery as a kinetic process, using two charge wells for the bound and available charges connected by a valve whose flow rate is proportional to the height difference between the wells [14].

[Equation that is referenced in the next section.] The change of charge in the wells is given by

$$\begin{cases} \frac{dy_1}{dt} = -I + k\left(h_2 - h_1\right) \\ \frac{dy_2}{dt} = -k\left(h_2 - h_1\right), \end{cases} \tag{1.2}$$

where y_1, y_2 are the charges, h_1, h_2 are the heights of the wells, the parameter k controls the rate of charge flow between the wells, and I is the applied load.

The flow rate of the valve should be lower than the typical discharge rate of the battery. During discharge from the available-charge well, the bound charges flow through the valve to equalize the heights of the two wells. It can be seen that for slower discharge rates, more charge flows through the valve and the effective capacity increases. Likewise, during idle periods for the battery, the available charge increases. Thus, the model is able to describe the rate-capacity and recovery effects.

1.2.3.3 Diffusion Model

Related to the kinetic battery model is the diffusion model, which describes the movement of the ions in the electrolyte of a lithium-ion battery [15]. Like in the kinetic battery model, the difference in the concentration of adjacent ions along the length of the battery determines the diffusion rate of the ions. The available charges are those ions directly touching the electrode of the battery. It can be seen that the kinetic battery model is a first-order approximation of the diffusion model [3], so naturally the diffusion model also describes the rate-capacity

and recovery effects.

1.2.4 Stochastic

Stochastic models describe the discharging and the recovery effect as stochastic processes. The first models were developed by Chiasserini and Rao and based on discrete-time Markov chains [16]. They studied two models of a battery in a communication device that transmitted packets. The simpler model described the battery as a discrete-time Markov chain with $N+1$ states, numbered from 0 to N and corresponding to the number of charge units available in the battery. Transmitting one packet requires one charge unit of energy. Thus, in continuous transmission, N packets can be sent. At every time step, a charge unit is either consumed with probability $a_1 = q$ or recovered with probability $a_0 = 1 - q$. The battery is considered empty when the 0 state is reached or when a theoretical maximum of T charge units have been consumed. The second model is an extension of the first, allowing for more than one charge unit to be consumed in a time step, modeling more bursty usage. Additionally, the battery has a non-zero probability of staying in the same charge state, indicating no consumption or recovery during a time step. Chiasserini and Rao extended their model further in following papers by adding state and phase dependence [2, 17, 18]. The state number is the number of charge units, and the phase number is the number of consumed charge units. Having fewer charge units decreases the probability of recovery, while having more consumed charge units increases the probability of recover. Using these models, one can model different loads by setting the transitions probabilities. However, the order of the transitions is uncontrollable, so it is impossible to model fixed load patterns and compute their impact on battery life.

Chiasserini and Rao mainly investigated the gain G in transmitted packets using a pulsed discharge relative to using a constant discharge, defined as $G = m/N$, where m is the mean number of transmitted packets. The gain increases when the load decreases, due to an

increase in the recovery probability. Additionally, the gain increases for lower discharge demand rates and higher current densities. These load profiles result in discharge currents close to the specified limits of the battery, causing the available capacity to decrease overly quickly. Therefore, the recovery effect is especially strong for these cases during pulsed discharge, greatly increasing the gain. Chiasserini and Rao compared the computation of the gain parameter for different current densities and demand rates using the stochastic model to that of the electrochemical model of Doyle et al. They found an average deviation of 1% and a maximum deviation of 4%. This shows that the stochastic model accurately describes battery behavior during pulsed discharge. However, this model is only able to compute relative lifetimes.

In 2005, Rao et al. [19] proposed a stochastic battery model based on the Kinetic Battery Model (KiBaM) of Manwell and McGowan. This stochastic KiBaM was for a nickel-metal hydride (NiMH) battery. The differential equations governing the original KiBaM were modified to include an extra factor h_2 governing the flow of charge between the wells. This changes Eq. (1.2) into

$$\begin{cases} \frac{dy_1}{dt} = -I + k_s h_2 \left(h_2 - h_1\right) \\ \frac{dy_2}{dt} = -k_s h_2 \left(h_2 - h_1\right), \end{cases} \tag{1.3}$$

This change causes the recovery effect to weaken as the remaining charge decreases. The stochastic model was also modified to allow the possibility of no recovery during idle periods. The stochastic KiBaM describes the battery using a discrete-time, transient Markov process. The states are labeled with the parameters (i, j, t), with i and j representing the discrete charge levels of the available and bound charge wells and t representing the length of the current idle period. Like the stochastic model of Chiasserini and Rao, it is impossible to fully model a real-life discharge pattern using the stochastic KiBaM. Rao et al. compared the results of their model with experimental results using an AAA NiMH battery. Two sets

of experiments were conducted, the first with varying frequency of the load and a 50% duty cycle and the second with varying off-time and a constant on-time. Their model accurately predicted the lifetime and delivered charge from the battery, with a maximum error of 2.65%.

1.2.5 Electrical-Circuit

One of the earliest investigations into using electrical circuits to represent batteries came about from a desire to represent impedance spectra created using electrochemical impedance spectroscopy (EIS). There are several major chemical processes within a battery with different time constants. Short-term processes include electric and magnetic, electric double layer, and mass transport effects; long-term processes include cyclical effects based on SOC, reversible effects such as acid stratification and memory effects, and the irreversible aging effect [20]. It is convenient to visualize the resultant complex spectra using a Nyquist plot, such as the one shown in Figure 1.1.As shown, the impedance can be divided into three parts, based on the frequency. The approximately linear low frequency portion, on the order of 10^{-6} to 10^{0} Hz, is caused by mass transport effects like diffusion. The middle frequency range, on the order of 10^{0} to 10^{3} Hz and in the shape of a semicircle, is caused by charge transfer and the electrochemical double layer effects. The remaining high frequency portion, on the order of 10^{3} to 10^{4} Hz, is a combination of the conductance and the skin effect.

In 1947, Randles proposed an equivalent electrical circuit to model interfacial electrochemical reactions [21]. His circuit, shown in Figure 1.2, consists of the electrolyte resistance R_s in series with the parallel combination of the double-layer capacitance C_{dl} and the impedance of the charge transfer resistance R_{ct} and the Warburg diffusion element Z_W. It is one of the simplest methods to interpret the results of EIS. Recently, Randles' circuit was used to study lithium-ion batteries.

In 1993, Hageman created simplified electrical-circuit models using PSpice for nickel-

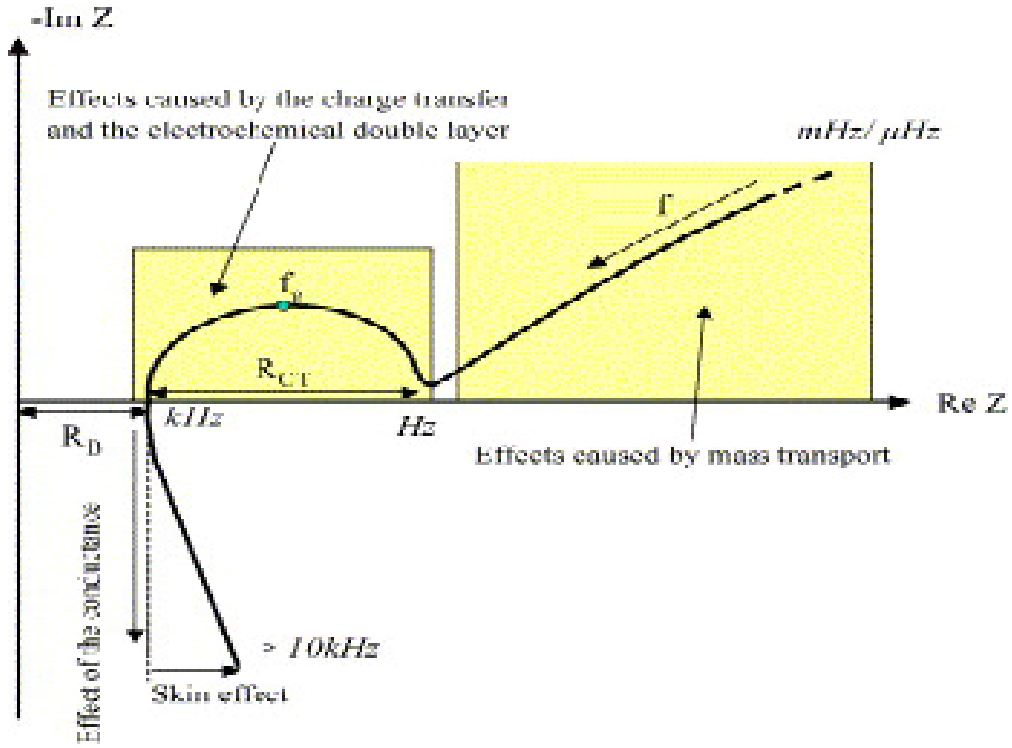

Figure 1.1. Illustrative Nyquist plot of a battery [20]. *[Quite low quality from screen capture of article preview. I can recapture for better quality or recreate it.]*

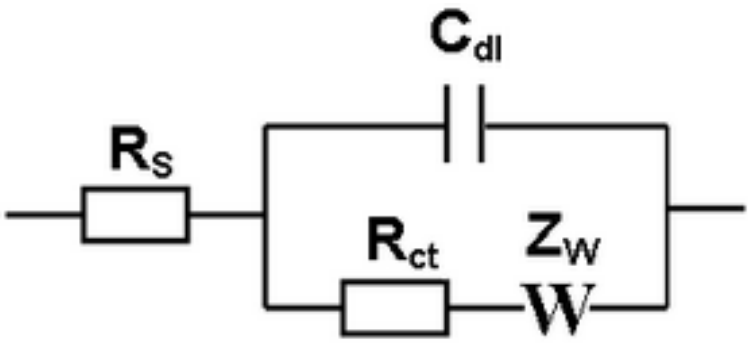

Figure 1.2. Randles' equivalent circuit.

cadmium (NiCd), lead-acid, and alkaline batteries [22]. The circuits shared the common elements of *i*) a capacitor that represents the battery capacity, *ii*) a discharge rate normalizer that determines the additional capacity loss at high discharge rates, *iii*) a circuit that discharges the battery, *iv*) a lookup table of battery voltage versus SOC, and *v*) a resistor that represents the battery's internal resistance [22, 23]. In addition, battery models for NiCd

batteries simulated the thermal effects under high discharge rates. The main lookup table is formed by discharging a battery at a low rate at a constant current (20 to 200 hours). At high discharge rates, the discharge rate normalizer reduces the battery voltage below the value from looking up the SOC in the table. This normalizer is implemented using additional lookup tables. These circuit models are much simpler than electrochemical models, but they are also less accurate with an approximately error of 10%. Furthermore, creation of the lookup tables requires considerable data.

Later on,

1.2.6 Evaluation

[24]

1.3 Nonlinear Filtering Methods

The battery model chosen for the purposes of this thesis has the advantage that it can be written in state-space form for use with commonly available state space filters. The rest of this section discusses the various nonlinear filtering techniques that can be applied to the model. [I have yet to read the paper.]

Chapter 2

Methodology

2.1 Battery Model

As discussed in the previous section, this thesis considers the electrical-circuit battery model proposed by Chen and Rincón-Mora [24] and shown in Figure 2.1. The left portion of the circuit models the capacity, SOC, and runtime, while the right portion models the transient i-v characteristics. For convenience, the model is designed so that the SOC of the battery equals the voltage V_{SOC}, in volts. The parameters C_{cap} and R_{sd} are assumed constant for a given battery and determine the capacity and self-discharge rate of the battery. The other parameters are all nonlinear functions of V_{SOC} and determine the transient i-v response as well as the open-circuit voltage V_{OC}. From a typical TCL PL-383562 polymer lithium-ion battery, Chen and Rincón-Mora extracted these parameters and fit them to curves, obtaining

$$R_s(V_{\mathrm{SOC}}) = 0.1562e^{-24.37V_{\mathrm{SOC}}} + 0.07446 \tag{2.1}$$

$$R_{ts}(V_{\mathrm{SOC}}) = 0.3208e^{-29.14V_{\mathrm{SOC}}} + 0.04669 \tag{2.2}$$

$$C_{ts}(V_{\mathrm{SOC}}) = -752.9e^{-13.51V_{\mathrm{SOC}}} + 703.6 \tag{2.3}$$

$$R_{tl}(V_{\mathrm{SOC}}) = 6.603e^{-155.2V_{\mathrm{SOC}}} + 0.04984 \tag{2.4}$$

$$C_{tl}(V_{\mathrm{SOC}}) = -6056e^{-27.12V_{\mathrm{SOC}}} + 4475 \tag{2.5}$$

$$V_{\mathrm{OC}}(V_{\mathrm{SOC}}) = -1.031e^{-35V_{\mathrm{SOC}}} + 3.685 + 0.2156V_{\mathrm{SOC}} - 0.1178V_{\mathrm{SOC}}^2 + 0.3201V_{\mathrm{SOC}}^3 \tag{2.6}$$

The resistance and capacitance parameters shown above are approximately constant for SOC > 0.2 and change exponentially for SOC < 0.2. The open-circuit voltage also changes exponentially for SOC < 0.2 but is approximately linear for SOC > 0.2. Note that the capacitances C_{ts} and C_{tl} are negative for very small SOC, while the experimental data collected by Chen and Rinón-Mora show that they stay positive. In order to correct this, the capacitances are held constant at the value given by some threshold SOC when below that threshold. These thresholds were determined experimentally and are SOC $= 0.006$ for C_{ts} and SOC $= 0.0115$ for C_{tl}.

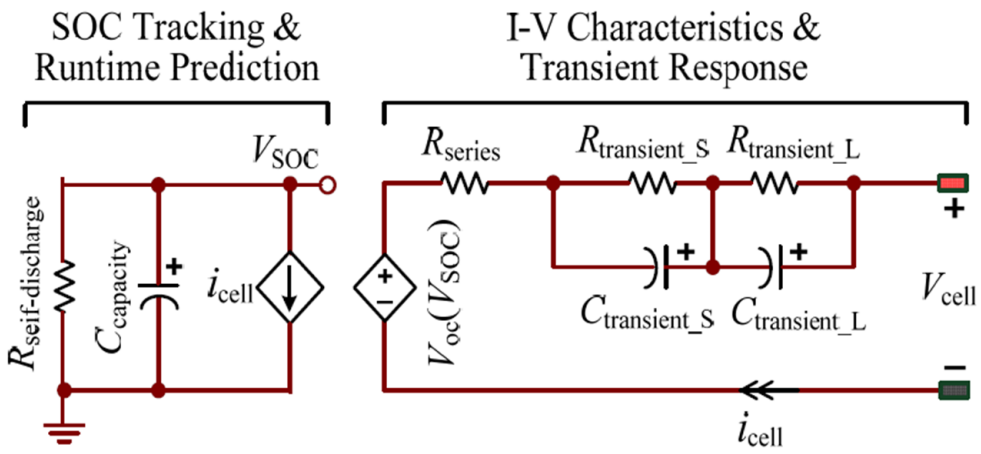

Figure 2.1. Battery model for simulation. [From paper, will redo later]

This study used the nonlinear parameters given by Chen and Rincón-Mora for the implementation of a battery using their battery model in Matlab. *The other, constant parameters were chosen to produce a capacity of 4 Ah and a self-discharge rate of 4% per month, assuming a nominal voltage of 3.7 V. [I didn't properly derive the following equations so my actual values are different.]* To do so, the equivalent capacitance C_{cap} to deliver the desired capacity

is calculated, and then the resistance R_{sd} that produces the desired self-discharge rate is calculated.

Some errors to be removed: More specifically, the capacitance C_{cap} is chosen to so that it supplies the same energy as a battery when discharged at

$$I_t\,[\text{A}] = C_n\,[\text{Ah}]/1\,[\text{h}], \tag{2.7}$$

where I_t is the discharge current in amperes, C_n is the rated capacity in ampere-hours, and n is the time base in hours for which the rated capacity is declared [25, 26]. Note that by definition, a fully charged battery with capacity C_n is fully discharged in n hours when discharged at a constant current of I_t/n [26]. The energy delivered by the battery over the $T = n$ hours is then

$$E_{\text{batt}} = \int_0^T V(t)I(t)\,\mathrm{d}t = T\left(\frac{1}{T}\int_0^T V(t)\,\mathrm{d}t\right)\frac{I_t}{n} = V_n I_t(1\,\text{h}) \tag{2.8}$$

$$= 3600 V_n I_t(\text{s})\,[\text{J}], \tag{2.9}$$

where V_n is the nominal voltage. The energy stored in the capacitor C_{cap} is $E_{\text{cap}} = C_{\text{cap}}V_{\text{SOC,max}}^2/2$. Recall that V_{SOC} has a maximum voltage of 1 V, so the capacitance needs to be

$$C_{\text{cap}} = 2E_{\text{batt}}/(1\,\text{V}^2) = 7200 V_n I_t(\text{s}/\text{V}^2)\,[\text{F}] \tag{2.10}$$

More specifically, the capacitance C_{cap} is chosen so that the charge it holds when V_{SOC} equals its maximum of 1 V is equivalent to the capacity of the battery. Therefore, for a given capacity of $C^\dagger$ in Ah, C_{cap} needs to be

$$C_{\text{cap}} = \frac{Q}{V_{\text{SOC}}} = \frac{C^\dagger}{1\ \text{V}} = 3600 C^\dagger\,[\text{F}]. \tag{2.11}$$

Then, the resistance R_{sd} is chosen so that the time constant $\tau = RC$ results in the desired drop of $\xi = 0.04$ over $T = 1$ month as follows

$$V(t) = V_0 e^{-T/\tau} = V_0(1 - \xi) \tag{2.12}$$

$$\tau = -T/\ln(1 - \xi) = -2592000/\ln 0.96\,[\text{s}]. \tag{2.13}$$

Then, $R_{sd} = \tau/C_{\text{cap}}$. Thus, the parameters are $C_{\text{cap}} = 14.4$ kF and $R_{sd} = 4409.4\ \Omega$. *[Actual values used in study are $C = 3789.5$ and $R = 6290.7$. That works out to 1052.6 mAh and 10.3% per month. Question is whether to change original setup or redo simulations.]*

For ease of filter design, it is useful to derive the state-space representation of the battery model. The physical variable definition is used, where the state variables are chosen to represent the stored charge in each capacitor. Choosing $x_1 = C_{ts}V_{ts}$, $x_2 = C_{tl}V_{tl}$, and $x_3 = C_{\text{cap}}V_{\text{SOC}}$, where the voltages are as defined in Figure 2.1, achieves the goal. Additionally, it can be seen that the cell current influences the state variables, while the cell voltage is influenced by them. Therefore, i_{cell} is defined as the state input and V_{cell} is defined as the state output. The resulting state space representation is

$$\dot{\mathbf{x}} = \begin{bmatrix} -1/R_{ts}C_{ts} & 0 & 0 \\ 0 & -1/R_{tl}C_{tl} & 0 \\ 0 & 0 & -1/R_{sd}C_{\text{cap}} \end{bmatrix} \mathbf{x} + \begin{bmatrix} 1 \\ 1 \\ -1 \end{bmatrix} i_{\text{cell}} \tag{2.14}$$

$$V_{\text{cell}} = V_{\text{OC}} - \frac{x_1}{C_{ts}} - \frac{x_2}{C_{tl}} - R_s i_{\text{cell}}. \tag{2.15}$$

While the above appears to be a linear system, remember that many of the parameters are functions of V_{SOC}, and thus, depend on the state x_3. Therefore, this is a nonlinear system.

In order to simulate the continuous-time system shown above, it is useful to convert the

system to discrete time. For a system with a sample period of T and a system in the form of

$$\begin{cases} \dot{x} = Ax + Bu \\ y = Cx + Du \end{cases}, \tag{2.16}$$

the discretization is $A_d = e^{AT}$ and $B_d = A^{-1}(A_d - I)B$ for nonsingular A, where I is the identity matrix. Note that A_d and B_d are functions of the SOC. For this nonlinear system, the most reliable numerical method of calculating the necessary exponential of a matrix was found through trial to be using the eigenvalues and eigenvectors. To do so, given a matrix A, the matrix exponent is

$$\textit{to add later} \tag{2.17}$$

The reliability of this method comes from the full set of eigenvectors resulting from the differing time constants in the system.

2.2 Filter Implementations

2.3 Simulation Setup

Determing the battery states is most difficult under high charge/discharge rates, for which the rate-capacity effect is the strongest. Additionally, idle periods following high currents produce strong recovery effects. Therefore, in order to create the most nonlinear behavior to test the filter performance, pulses were used to charge and discharge the simulated battery. Initially, the battery starts fully discharged and stays idle for 900 s. Then, it is charged to full by charging at 0.25 A for 1900 s. Next, six cycles of discharging and charging are conducted. Each cycle lasted for 28000 s. The pulses had an on-time of 1450 s and an off-time of 1350 s at a current of 0.25 A. It is assumed that the simulated battery has circuitry that keeps the

SOC within its limits of zero and one by changing the current flow. This was implemented by a current control scheme that changed the current to the self-discharge rate whenever charging of a full battery or discharging of an empty battery occured.

Because of the possibility of the activation of the current control scheme, it is necessary to first determine the actual current as related to the capacity change within the battery. To do so, the SOC was simulated using the left part of the battery model at various sample rates for the described current, with the described current control scheme, using the `ode45` solver in Matlab 2013a. To ensure convergence, the max time step was set to the one-tenth of the pulse period. Additionally, the relative and absolute tolerances were reduced to 10^{-6} and 10^{-10}, respectively, for the same reason. The SOC was found at the sample times using linear interpolation. Afterwards, the numerical central difference of the SOC voltage is found to determine when the current control scheme was active. Then, the current was adjust using this information to represent the actual capacity change within the battery. This adjusted current was used to calculate the actual SOC analytically, since the left circuit is a LTI system. Following this, the parameters of the right part of the circuit can be calculated as a function of SOC. That part of the system was simulated assuming cubic interpolation of the parameter values using the ode15s solver with relative and absolute tolerances of 10^{-6} and 10^{-10}. The solver and tolerances were chosen to achieve good accuracy for the stiff system. Finally, the battery voltage is calculated using the states of the right-hand circuit.

The simulated current and voltage have white Gaussion noise added to them to simulate additive measurement noise.

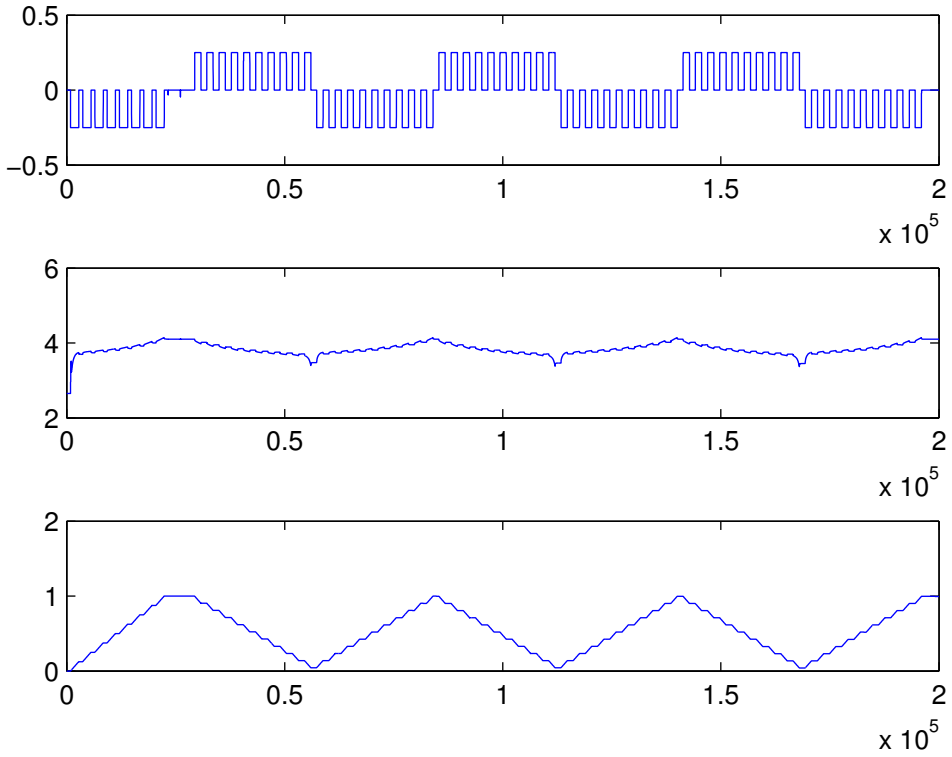

Figure 2.2. Discharge current along with the resulting voltage and SOC.

Bibliography

[1] D. Doerffel and S. A. Sharkh, "A critical review of using the peukert equation for determining the remaining capacity of lead-acid and lithium-ion batteries," *Journal of Power Sources*, vol. 155, no. 2, pp. 395–400, 2006.

[2] C. F. Chiasserini and R. R. Rao, "A model for battery pulsed discharge with recovery effect," in *Wireless Communications and Networking Conference, 1999. WCNC. 1999 IEEE*, vol. 2, 1999, pp. 636–639.

[3] M. R. Jongerden and B. R. Haverkort, "Which battery model to use?" *IET Software*, vol. 3, no. 6, pp. 445–457, Dec. 2009.

[4] M. Doyle, T. F. Fuller, and J. Newman, "Modeling of galvanostatic charge and discharge of the lithium/polymer/insertion cell," *Journal of the Electrochemical Society*, vol. 140, no. 6, pp. 1526–1533, 1993.

[5] T. F. Fuller, M. Doyle, and J. Newman, "Simulation and optimization of the dual lithium ion insertion cell," *Journal of the Electrochemical Society*, vol. 141, no. 1, pp. 1–10, 1994.

[6] ——, "Relaxation phenomena in lithium-ion insertion cells," *Journal of the Electrochemical Society*, vol. 141, no. 4, pp. 982–990, 1994.

[7] J. Newman, *Fortran programs for the simulation of electrochemical systems*, `http://www.cchem.berkeley.edu/jsngrp/fortran.html`, 1998.

[8] J. C. Bezdek, "On the relationship between neural networks, pattern recognition and intelligence," *International Journal of Approximate Reasoning*, vol. 6, no. 2, pp. 85–107, 1992.

[9] ——, "What is computational intelligence?" In *Computational Intelligence: Imitating Life*, J. M. Zurada, R. J. Marks, and C. J. Robinson, Eds., IEEE Press, 1994, pp. 1–12.

[10] C. C. O'Gorman, D. Ingersoll, R. G. Jungst, and T. L. Paez, "Artificial neural network simulation of battery performance," in *Proceedings of the Thirty-First Hawaii International Conference on System Sciences*, vol. 5, Jan. 1998, pp. 115–121.

[11] G. Capizzi, F. Bonanno, and G. M. Tina, "Recurrent neural network-based modeling and simulation of lead-acid batteries charge-discharge," *IEEE Transactions on Energy Conversion*, vol. 26, no. 2, pp. 435–443, Jun. 2011.

[12] J. Wang, Q. Chen, and B. Cao, "Support vector machine based battery model for electric vehicles," *Energy Conversion and Management*, vol. 47, no. 7–8, pp. 858–864, 2006.

[13] W. X. Shen, C. C. Chan, E. W. C. Lo, and K. T. Chau, "Adaptive neuro-fuzzy modeling of battery residual capacity for electric vehicles," *IEEE Transactions on Industrial Electronics*, vol. 49, no. 3, pp. 677–684, Jun. 2002.

[14] J. F. Manwell and J. G. McGowan, "Lead acid battery storage model for hybrid energy system," *Solar Energy*, vol. 50, no. 5, pp. 399–405, 1993.

[15] D. N. Rakhmatov and S. B. K. Vrudhula, "An analytical high-level battery model for use in energy management of portable electronic systems," in *Proceedings of the 2001 IEEE/ACM International Conference on Computer-aided Design*, ser. ICCAD '01, San Jose, California: IEEE Press, 2001, pp. 488–493.

[16] C. F. Chiasserini and R. R. Rao, "Pulsed battery discharge in communication devices," in *Proceedings of the 5th Annual ACM/IEEE International Conference on Mobile Computing and Networking*, ser. MobiCom '99, 1999, pp. 88–95.

[17] ——, "Improving battery performance by using traffic shaping techniques," *IEEE Journal on Selected Areas in Communications*, vol. 19, no. 7, pp. 1385–1394, 2001.

[18] ——, "Energy efficient battery management," *IEEE Journal on Selected Areas in Communications*, vol. 19, no. 7, pp. 1235–1245, 2001.

[19] V. Rao, G. Singhal, A. Kumar, and N. Navet, "Battery model for embedded systems," in *Proceedings of the 18th International Conference on VLSI Design held jointly with 4th International Conference on Embedded Systems Design*, ser. VLSID '05, Washington, DC, USA: IEEE Computer Society, 2005, pp. 105–110.

[20] A. Jossen, "Fundamentals of battery dynamics," *Journal of Power Sources*, vol. 154, no. 2, pp. 530–538, 2006.

[21] J. E. B. Randles, "Kinetics of rapid electrode reactions," *Discussions of the Faraday Society*, vol. 1, pp. 11–19, 1947.

[22] S. C. Hageman, "Simple PSpice models let you simulate common battery types," *Electronic Design News*, vol. 38, pp. 117–129, 1993.

[23] ——, "Using PSpice to simulate the discharge behavior of common batteries," in *MicroSim Application Notes*, ver. 8.0, MicroSim Corporation, 1997, pp. 260–286.

[24] M. Chen and G. A. Rincón-Mora, "Accurate electrical battery model capable of predicting runtime and i-v performance," *IEEE Transactions on Energy Conversion*, vol. 21, no. 2, pp. 504–511, Jun. 2006.

[25] IEC SC 21A, "Secondary cells and batteries containing alkaline or other non-acid electrolytes – guide to designation of current in alkaline secondary cell and battery standards," The International Electrotechnical Commission, Tech. Rep. IEC 61434, 1996.

[26] D. Linden, "Factors affecting battery performance," in *Handbook of Batteries*, D. Linden and T. B. Reddy, Eds., 3rd ed., McGraw-Hill, 2001, ch. 3.